Zeeman splitting in GaInNAs

2004 J. Phys.: Condens. Matter 16 S3319

(http://iopscience.iop.org/0953-8984/16/31/021)

INSTITUTE OF PHYSICS PUBLISHING JOURNAL OF PHYSICS: CONDENSED MATTER

J. Phys.: Condens. Matter **16** (2004) S3319–S3331 PII: S0953-8984(04)75684-2

Zeeman splitting in GaInNAs

C Skierbiszewski[1] **and J Łusakowski**[2]

[1] High Pressure Research Center Unipress, Sokołowska 29/37, 01-142 Warsaw, Poland
[2] Institute of Experimental Physics, Hoża 69, 00-681 Warsaw, Poland

Received 2 February 2004
Published 23 July 2004
Online at stacks.iop.org/JPhysCM/16/S3319
doi:10.1088/0953-8984/16/31/021

Abstract

We carried out magneto-absorption and Faraday rotation experiments to investigate the Zeeman splitting in GaInNAs alloys. We determined the effective g^*-factors for the fundamental transition $\Gamma_8 \rightarrow E_-$, as well as for higher energy transitions $\Gamma_8 \rightarrow E_+$ and $\Gamma_7 \rightarrow E_-$. The following experimental values of the electron and hole g-factors in $Ga_{0.96}In_{0.04}N_{0.01}As_{0.99}$ were obtained: $g^*_{E-} = -0.7 \pm 0.2$, $g^*_{E+} = +2.8 \pm 0.8$, $g^*_{\Gamma 8} = -1.6 \pm 0.2$ and $g^*_{\Gamma 7} = -4.9 \pm 0.6$ for the E_-, E_+, Γ_8 and Γ_7 band, respectively. The electron effective g-factor for the E_- band was studied in detail as a function of N and In content. Oscillations of the Faraday rotation angle allowed us to determine the electron effective mass at the bottom of the conduction band for $Ga_{0.96}In_{0.04}N_{0.01}As_{0.99}$, $m^*_e = 0.086\, m_0$.

1. Introduction

GaInNAs compounds belong to a new class of materials where the addition of a few per cent of nitrogen significantly changes the conduction band (CB) structure, leading to several unexpected effects. A reduction of the band gap energy as large as 0.18 eV was observed in GaNAs for 1% of N [1]. Nitrogen-induced splitting of the CB (to the E_- and the E_+ bands) was observed in photomodulation spectroscopy in reflection geometry [2] as well as in absorption [3, 4] experiments (see figure 1). A drastic increase of the electron effective mass and a large nonparabolicity was experimentally detected [5]. Since the addition of indium to GaNAs compensates a lattice contraction induced by nitrogen atoms and also reduces the energy gap, it is possible to grow quaternary GaInNAs layers with a different energy gap and lattice matched to a GaAs substrate (to this aim, the In to N ratio should be equal to about 3:1). This opens new perspectives for optoelectronic applications and generates a considerable interest in a theoretical description of the band structure of this class of materials.

Shan and Walukiewicz proposed the Band Anticrossing phenomenological model [2] that explains major peculiarities of the CB of III–N–V compounds on the basis of an interaction

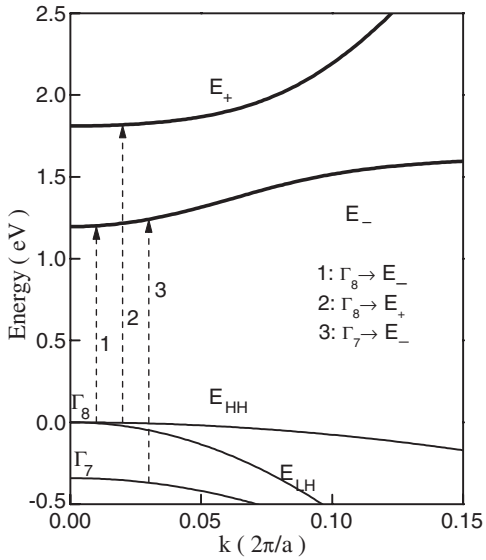

Figure 1. Conduction band splitting and dispersion in GaInNAs. The arrows indicate different optical transitions discussed in the text.

between localized states of the A_1 symmetry related to nitrogen atoms and conduction band states of the host matrix (GaAs, GaInAs or GaAlAs). In other words, this model assumes an admixture of N-related states to the CB states. On the other hand, *ab initio* calculations revealed quite a different role of the nitrogen atoms. Their presence causes breaking of the T_d symmetry of the lattice and leads to a mixing of the Γ, X and L bands without any significant admixture of N-related states [6–9]. Both approaches predict qualitatively similar CB nonparabolicity [4, 9], interband transition oscillator strengths and band positions. An intense debate on the microscopic origin of the structure of the CB of GaNAs and GaInNAs and the role played by N in its formation is still going on [10, 11]. Experimental and theoretical studies revealed that N predominantly modifies the CB structure. In our previous work we found that the addition of nitrogen atoms mainly changes the structure of the CB without affecting the positions of the valence bands (the valence band spin–orbit splitting energy remains unchanged [4]).

Up to now, there are no experimental results or theoretical evaluations concerning the effective g-factors in GaInNAs alloys. It would be highly interesting (e.g., for a theoretical description) to compare g-factors for the E_+ and the E_- bands. We would like partially to cover this gap by reporting for the first time the Zeeman splitting and Landé effective g^*-factors for both the E_- and the E_+ conduction bands as well as for the Γ_8 and the Γ_7 valence bands of $Ga_{0.96}In_{0.04}N_{0.01}As_{0.99}$. For the fundamental transition, $\Gamma_8 \rightarrow E_-$, we studied the effective g^*-factor as a function of N and In content. The values of Landé g^*-factors are deduced from (a) measurements of magneto-absorption of the circularly polarized light in the Faraday configuration, and (b) an investigation of the rotation of the linearly polarized light in the Faraday rotation (FR) experiment. In the latter case, the oscillations of the angle of rotation of the polarization plane were observed at energies above the band edge that resemble optical Shubnikov–de Haas oscillations resulting from quantization of the bands into the Landau levels. Carrying out measurements as a function of the magnetic field strength allowed the determination of the electron–hole reduced effective mass.

Let us recall that in an external magnetic field, B, the two-fold spin degenerated CB is described by

$$E_c = E_0 + (n + \tfrac{1}{2})\hbar\omega_c + sg_e^*\mu_B B, \tag{1}$$

where n is the Landau level quantum number, s is the electron spin quantum number ($s = \pm 1/2$), μ_B is the Bohr magneton, $\omega_c = eB/m_e^*$ is the cyclotron frequency with m_e^* the electron effective mass, and g_e^* is the g-factor of the electron moving in the CB.

For GaAs, the experimentally determined g_e^* equals -0.44 ± 0.02 at 5 K, and it becomes less negative at higher temperatures [12]. For $Ga_{1-x}In_xAs$ compounds, the electron g-factor decreases with In content, $g_e^* = -0.44 - 3.6x$ (for $x < 0.1$) [13]. It follows from theoretical studies that the major contribution to g_e^* in GaAs comes from the spin–orbit coupling, as $k \cdot p$ calculations within three- or five-band approximation show [14–16]. The g-factor for the Γ_8 valence band of GaAs was deduced from an FR experiment [17], where the sum of the electron and the hole g-factors was determined: $g^* = g_e^* + g_{\Gamma 8}^* = -2.1$. The g-factor for the Γ_7 valence band, $g_{\Gamma 7}^* = -4.9 \pm 1$, was obtained from stress-modulated magneto-reflectivity measurements [18].

2. Experimental details

The $Ga_{1-y}In_yN_xAs_{1-x}$ samples used in this study were grown by either metal-organic-vapour-deposition (MOCVD) or by molecular beam epitaxy (MBE). The thin films were closely lattice matched to GaAs substrates by maintaining the In to N composition ratio $y \sim 3x$. In order to measure the absorption coefficient in a wide photon energy range, a specially designed structure was grown that allowed separation of the layer from the substrate. The structure consists of a 0.1 μm thick GaAs buffer (grown on a semi-insulating GaAs substrate) followed by a 100 nm thick GaAlAs etch stop layer, and then by a 1.87 μm thick $Ga_{0.96}In_{0.04}N_{0.01}As_{0.99}$ layer. The details of crystal growth and sample preparation are given elsewhere [4, 19, 20].

The magneto-absorption and the FR experiments were carried out in an optical cryostat supplied with a 6 T superconducting split coil and a spectrometer with a charged coupled device (CCD) detector. The samples were immersed directly in the pumped liquid helium at $T = 2$ K and their surface was perpendicular to the direction of the magnetic field. A beam of the incident light (polarized linearly in the FR experiment and polarized circularly in the magneto-absorption experiment) was directed parallel to the magnetic field. The angle of the FR was determined as a function of the energy by turning a quartz linear polarizer introduced into the light beam between the sample and the spectrometer. This polarizer was supplied with a Fresnel $\lambda/4$ rhomb in the magneto-absorption experiment and both circular polarizations were detected by inversion of the magnetic field.

3. Results

Figure 2 shows the absorption coefficient of GaInNAs for circularly polarized light, α^+, for magnetic field strengths of $B = 5$ and -5 T, respectively. This type of experiment is equivalent to measurements of absorption coefficient of right, α^+, and left, α^-, circularly polarized light without changing the orientation of the magnetic field. As is shown in the inset, there is a small energy shift between these spectra; it is a signature of the spin splitting of the conduction and the valence band induced by the magnetic field. The energy shift, ΔE, between the two spectra is given by

$$\Delta E = (g_e^* + g_v^*)\mu_B B, \tag{2}$$

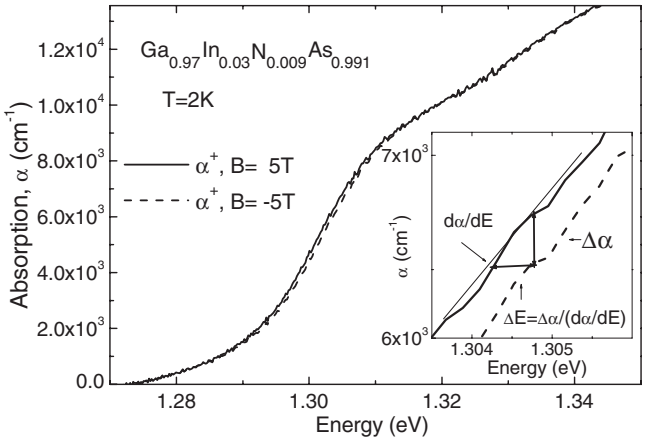

Figure 2. The absorption coefficient of circularly polarized light, $\alpha(E)$, in GaInNAs for magnetic field strengths of 5 and −5 T, respectively. The inset shows the Zeeman splitting of the fundamental transition.

where g_e^* and g_v^* are g-factors describing the spin splitting of the CB (E_-) and the valence band (Γ_8), respectively.

A direct determination of ΔE from the positions of the absorption edges α^+ (5 T) and α^+ (−5 T) is rather difficult because the band edge is not very sharp (see figure 2). Figure 3 presents the method of determination of ΔE with a higher accuracy. ΔE is calculated according to the following expression (see the inset to figure 2):

$$\Delta E = \frac{\alpha^+(B) - \alpha^+(-B)}{\mathrm{d}\alpha^+/\mathrm{d}E}, \tag{3}$$

where $\mathrm{d}\alpha^+/\mathrm{d}E$ is the derivative of the absorption coefficient.

We calculated the difference between the absorption coefficients for two directions of the magnetic field (figure 3(b)) and divided it by the slope coefficient (the first derivative of the absorption coefficient, α; see figure 3(c)). In figure 3(d) we show the energy separation, ΔE. For energies around 1.3 eV, i.e., in the energy range corresponding to the maximum splitting between the absorption edges α^+ (5 T) and α^+ (−5 T), the value of $|\Delta E|$ is 0.64 ± 0.05 meV, as shown by the thick solid line. Application of this procedure to samples with different nitrogen content allows plotting the data presented in figure 4, which shows the splitting of the fundamental band edge in the magnetic field (solid dots). The corresponding In content is indicated near each experimental point. The square symbol in figure 4 shows the value obtained for GaAs in [17] ($g_{\mathrm{eff}}^* = g_e^* + g_v^* = -2.1$). We will consequently assume that the energy splitting of the fundamental transition in GaInNAs compounds, in the range where the N and In content is of interest, is described by a negative effective g-factor, g_{eff}^*, as it is in the case of GaAs. The sign of ΔE was deduced from the fact that it is negative for GaAs, and in the case of GaInNAs with low N and In content, the main contribution to g_{eff}^* comes from the negative valence band g-factor, g_v^*.

To have some insight to the effective g-factors for other transitions, we performed similar experiments on a thin (1.87 μm) $Ga_{0.96}In_{0.04}N_{0.01}As_{0.99}$ layer in a wide range of energies (from 1.2 up to 2 eV). This layer was attached to a sapphire holder with glue. In figure 5 we present the absorption spectra (figure 5(a)) together with $\Delta\alpha(E)$ and $\mathrm{d}\alpha^+/\mathrm{d}E$. For clarity, we multiplied $\Delta\alpha$ by a factor of five in the energy range 1.7–2 eV. We would like to underline two striking features visible in $\Delta\alpha(E)$ plot:

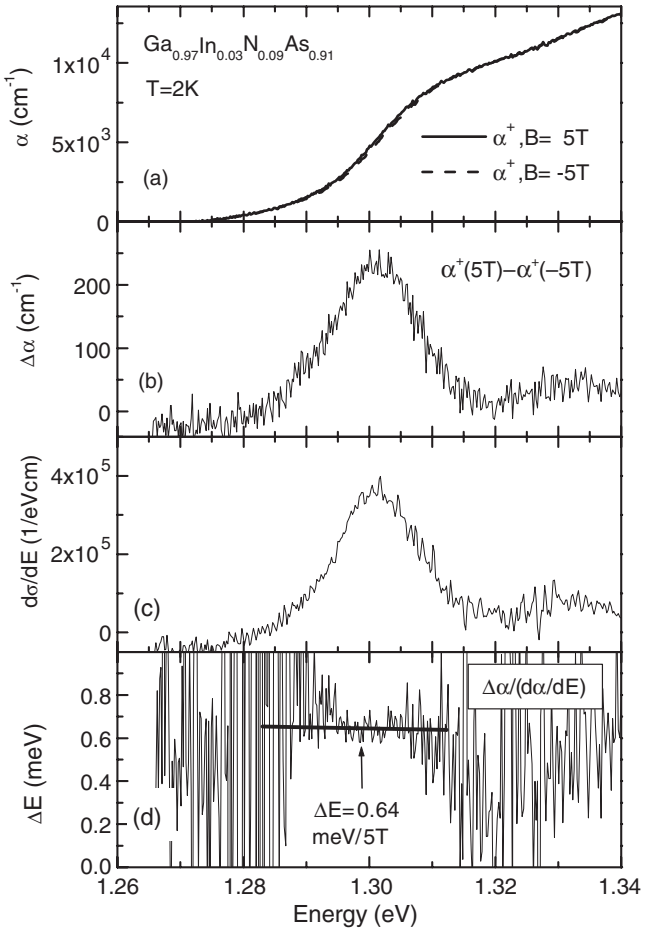

Figure 3. (a) The absorption coefficient of circularly polarized light, $\alpha(E)$, in GaInNAs for magnetic field strengths of 5 and −5 T, respectively. (b) The difference between the circularly polarized light absorption coefficient, $\Delta\alpha(E)$, for 5 and −5 T. (c) The derivative of the absorption coefficient. (d) The Zeeman splitting.

(I) $\Delta\alpha$ around 1.87 eV (for the transition $\Gamma_8 \rightarrow E_+$) has the opposite sign in comparison with $\Delta\alpha$ for transitions around 1.3 eV ($\Gamma_8 \rightarrow E_-$) and 1.64 eV ($\Gamma_7 \rightarrow E_-$). This means that the g-factor for E_+ has the opposite sign to that for E_-.

(II) For the fundamental transition around 1.3 eV, oscillations of $\Delta\alpha$ appear. We expand this energy range in figure 6. The energy distances between subsequent minima are the same, which indicates that the oscillations are due to the Landau level splitting of the conduction and valence bands. We will discuss this effect in more detail below.

To investigate the influence of the magnetic field on the Zeeman splitting and oscillation effects for the $\Gamma_8 \rightarrow E_-$ transition, we performed FR experiments. The FR angle for different magnetic fields is plotted in figure 7. We observe an increase of the amplitude of the FR angle with the magnetic field. Similarly to the magneto-absorption experiment, oscillations in the FR spectra are observed. The distance between subsequent maxima exhibited in the spectra in figure 7 depends linearly on the magnetic field.

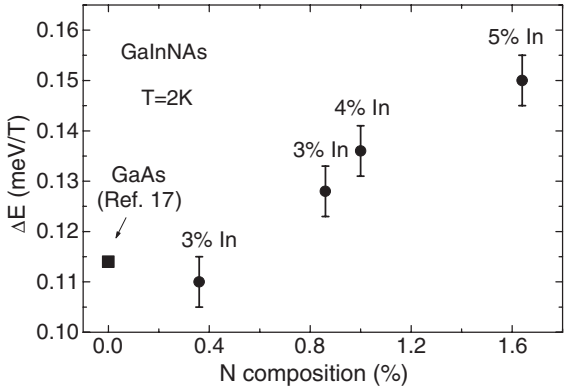

Figure 4. The energy dependence of the Zeeman splitting, ΔE, in GaInNAs for different N and In content (dots). The indium mole fraction is indicated for each experimental point. The square shows ΔE after [17].

4. Discussion

4.1. Analysis of the Faraday rotation experiments

In the FR experiments, the rotation of the polarization plane of the incident light, Θ_{FR}, measured versus the energy, E, depends on the difference between the refractive indices, $n_{\pm}$, for the right and the left circularly polarized light:

$$\Theta_{\mathrm{FR}}(E) = \frac{dE}{2\hbar c}\left[n_{+}(E) - n_{-}(E)\right], \tag{4}$$

where d is the sample thickness; $\hbar$ and c have their usual meaning. The refractive index n is related to the absorption coefficient $\alpha(E)$ through the Kramers–Kröning relation

$$n(E) - 1 = \frac{c\hbar}{\pi} P \int_0^{\infty} \frac{\alpha(x)}{x^2 - E^2}\,\mathrm{d}x, \tag{5}$$

and the difference of the refractive indices can be calculated from the following equation:

$$n_{+}(E) - n_{-}(E) = \frac{c\hbar}{\pi}\left[P\int_0^{\infty}\frac{\alpha(x)}{x^2-E^2}\,\mathrm{d}x - P\int_0^{\infty}\frac{\alpha(x+\Delta E)}{x^2-E^2}\,\mathrm{d}x\right]. \tag{6}$$

To model the $\Theta_{\mathrm{FR}}(E)$ dependence one could use in equation (6) an analytical formula for $\alpha(E)$, if a particular model of the band edge is assumed (i.e., direct, excitonic, etc). In the case of the present study, $\alpha(E)$ was measured independently, and the experimental data were used to derive $\Theta_{\mathrm{FR}}(E)$. The dots in figure 8 show the FR experimental results for $B = 2$ T. The solid curve is the theoretical fit described above (with $\Delta E = 0.26$ meV).

The Zeeman splitting, ΔE, for the $\Gamma_8 \rightarrow \mathrm{E}_-$ transition as a function of the magnetic field strength is plotted in figure 9. The linear behaviour of ΔE versus B indicates that the effective g-factor does not depend on the magnetic field strength. The nonlinear dependence of an effective g-factor on B observed in GaAs (in magnetic fields up to 5 T) was explained in terms of mixing of the light and heavy hole valence bands [21, 22]. In our case, the linear dependence of ΔE on B suggests that the degeneracy of the valence band at the Γ_8 point is already lifted, and the light and heavy holes originating from the Γ_8 valence band are energetically separated. Such an effect can occur when a strain (e.g., biaxial) is applied to a layer, and this phenomenon is widely used to decrease the operation threshold of GaAs-based lasers. In the case of the present study, a possible explanation of the presence of a strain in the layer lies in the procedure of sample preparation. To recover the thin GaInNAs layer itself,

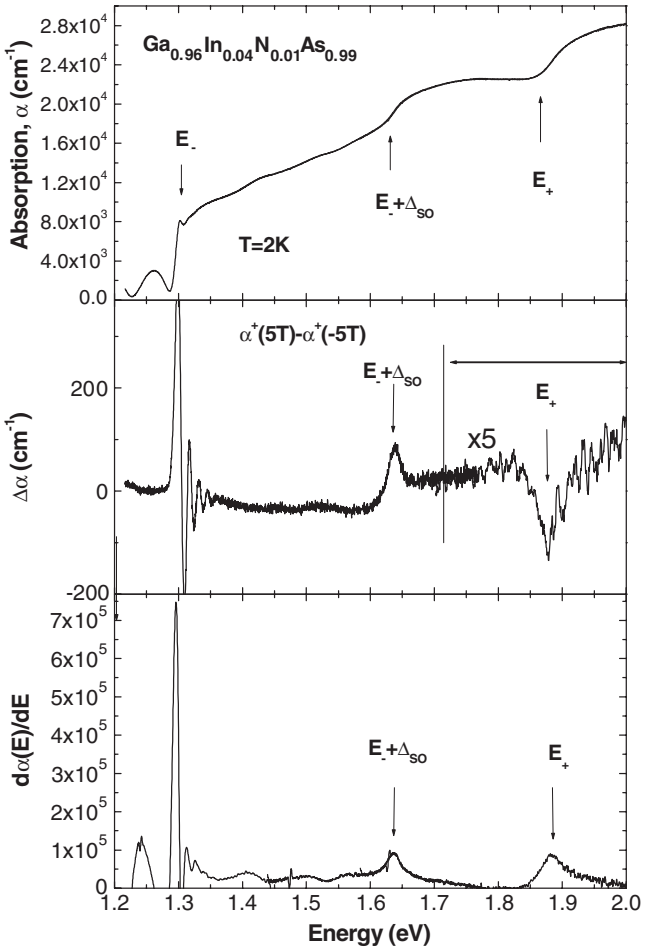

Figure 5. (a) The absorption coefficient of a thin $Ga_{0.96}In_{0.04}N_{0.01}As_{0.99}$ layer. The positions of the energy gap E_-, transition from the Γ_7 valence band to the E_-, $(E_- + \Delta_{SO})$ band and transition from the Γ_8 to the E_+ for GaInNAs are indicated by the arrows. (b) The difference of the absorption coefficient for 5 and −5 T. (c) The derivative of the absorption coefficient.

the sample was glued to the sapphire at room temperature, and the substrate was removed by etching. At helium temperatures, due to the difference in thermal expansion coefficients between GaInNAs and sapphire, the thin layer is strained. This can lead to a separation of the light and the heavy hole bands. We verified this hypothesis by performing measurements on a layer glued on sapphire and a reference layer deposited on a GaAs substrate (see figure 6). The magneto-absorption spectra for the free standing layer was red-shifted (by 1 meV, suggesting the energy gap shrinkage due to an additional strain) in comparison to the sample on the GaAs substrate. To conclude, the linear dependence of the Zeeman effect versus the magnetic field is indicative for a $\Gamma_8 \rightarrow E_-$ optical transition from the light hole valence band.

4.2. The effective g-factor for the E_- conduction band

In our experiments, we determined the effective $g^*_{\rm eff}$-factor that is the sum of the electron and hole g-factors, $g^*_{\rm eff} = g^*_{\rm e} + g^*_{\rm v}$. In table 1 we have collected data resulting from measurements of the $\Gamma_8 \rightarrow E_-$ optical transition. We have shown already, that the presence of nitrogen

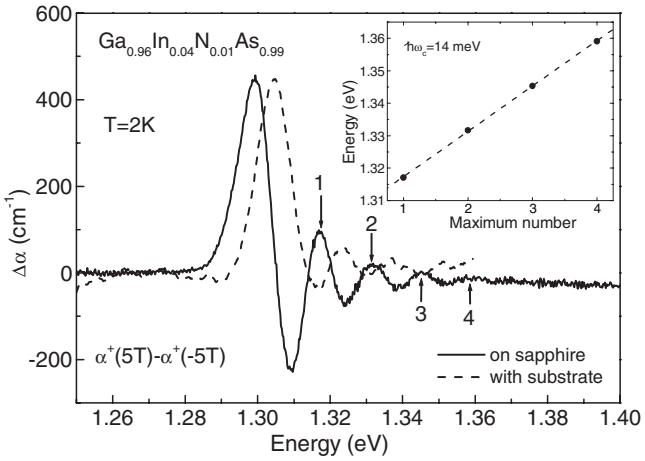

Figure 6. The difference of the absorption coefficient for 5 and −5 T for the fundamental transition in $Ga_{0.96}In_{0.04}N_{0.01}As_{0.99}$: solid curve—a thin layer glued on sapphire (removed from a GaAs substrate); dashed curve—a reference layer on a GaAs substrate. The arrows indicate positions where the energy of interband transitions fits to the energy of the valence and conduction band Landau level system. The inset shows positions of minima of the difference of the absorption coefficient as a function of the minimum number. The slope of the line allows us to estimate the reduced effective mass.

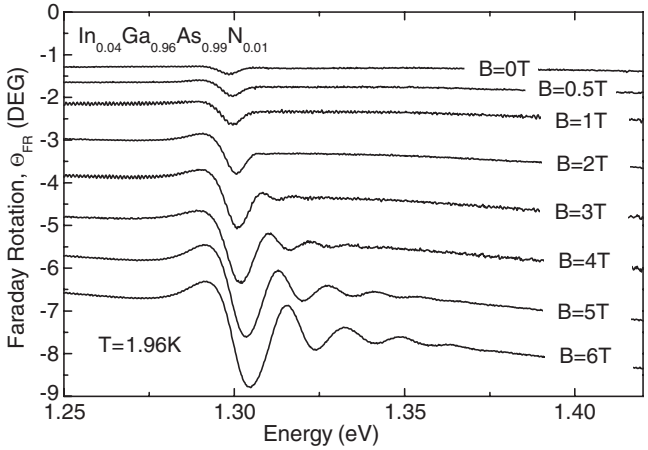

Figure 7. The Faraday rotation angle for different magnetic fields for the $Ga_{0.96}In_{0.04}N_{0.01}As_{0.99}$ layer. Plots for different magnetic field are shifted.

does not affect the valence bands: for example, the valence-band spin–orbit splitting does not depend on N content [4]. This enables us to assume that g_v^* does not depend on N (up to 1.6%) and In (up to 5%) content and $g_v^* = -1.6$ (i.e., is equal to that for GaAs; see [12] and [17]). The dots in figure 10 present the values of the effective electron g-factor for the E_- band, g_{E-}^*, extracted from the Zeeman splitting in GaInNAs. We observe a monotonic decrease of g_{E-}^* with nitrogen content that cannot be attributed solely to the presence of indium in the layers. The influence of In itself on the electron effective g-factor in GaInAs is plotted by open squares, after [13]. The presence of nitrogen in GaInNAs further decreases the value of the electron g-factor.

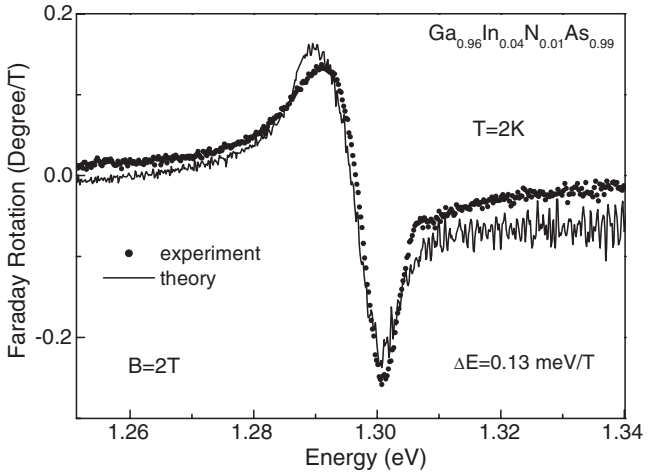

Figure 8. The Faraday rotation angle as a function of energy for the $Ga_{0.96}In_{0.04}N_{0.01}As_{0.99}$ layer at 2 T (dots). The solid curve shows the numerical evaluation with Zeeman splitting $\Delta E = 0.26$ meV and the absorption coefficient shown in figure 5(a).

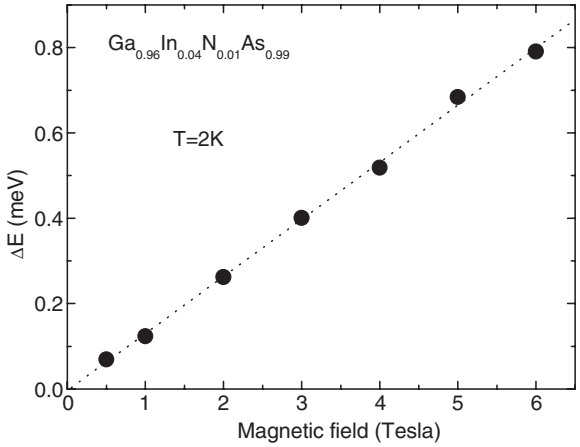

Figure 9. The Zeeman splitting for the $\Gamma_8 \rightarrow E_-$ optical transition from the Faraday rotation measurements as a function of magnetic field.

Table 1. Zeeman splitting, ΔE, and the effective g-factor, $g_e^* + g_v^*$, for the fundamental transition in GaInNAs with different In and N content.

N content (%)	In content (%)	ΔE (meV T^{-1})	$g_e^* + g_v^*$
0.4	3	-0.11 ± 0.01	-1.9 ± 0.2
0.9	3	-0.128 ± 0.01	-2.2 ± 0.2
1	4	-0.132 ± 0.01	-2.3 ± 0.2
1.6	5	-0.15 ± 0.01	-2.6 ± 0.2

4.3. The g-factors in GaInNAs for the conduction and the valence bands*

In table 2 the experimental data resulting from the Zeeman splitting for different optical transitions for $Ga_{0.96}In_{0.04}N_{0.01}As_{0.99}$ are presented. From table 2 we can deduce the difference

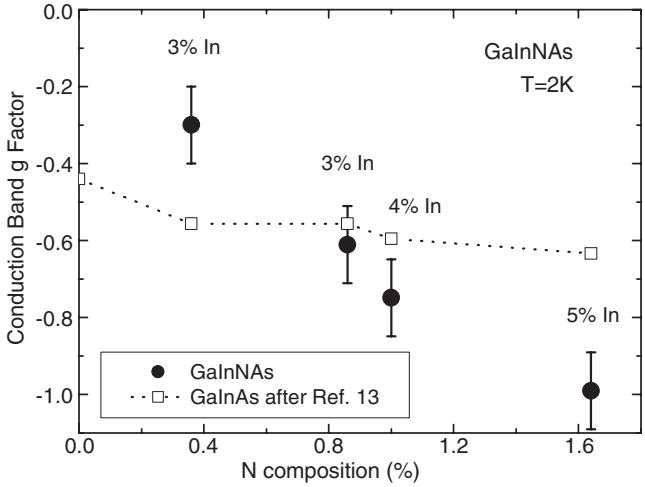

Figure 10. The conduction band g-factor for GaInNAs calculated with the assumption that the g-factor for the Γ_8 valence band is equal to -1.6. The open squares show the behaviour of the conduction band g-factor for GaInAs after [13].

Table 2. Zeeman splitting, ΔE, and the effective g-factor, $g_e^* + g_v^*$, for different optical transitions observed in magneto-absorption experiments in $Ga_{0.96}In_{0.04}N_{0.01}As_{0.99}$.

Optical transition	ΔE (meV T^{-1})	$g_e^* + g_v^*$
$\Gamma_8 \rightarrow E_-$	-0.136 ± 0.01	-2.3 ± 0.2
$\Gamma_7 \rightarrow E_-$	-0.33 ± 0.02	-5.6 ± 0.4
$\Gamma_8 \rightarrow E_+$	$+0.07 \pm 0.03$	$+1.2 \pm 0.6$

Table 3. Effective g-factors in $Ga_{0.96}In_{0.04}N_{0.01}As_{0.99}$ for the conduction E_- (g^*_{E-}), E_+ (g^*_{E+}) and valence Γ_7 ($g^*_{\Gamma 7}$), Γ_8 ($g^*_{\Gamma 8}$) bands, determined with the assumption that $g^*_{\Gamma 8}$ is equal to -1.6 (i.e., the same as for GaAs).

Effective g^* factors in $Ga_{0.96}In_{0.04}N_{0.01}As_{0.99}$	
g^*_{E-}	-0.7 ± 0.2
g^*_{E+}	$+2.8 \pm 0.8$
$g^*_{\Gamma 8}$	-1.6 ± 0.2
$g^*_{\Gamma 7}$	-4.9 ± 0.6

between the electron g-factors for E_+ and E_- bands: $g^*_{E+} - g^*_{E-} = 3.5 \pm 0.8$. Taking $g^*_{\Gamma 8} = -1.6$, we can calculate the effective g-factors for the Γ_7, E_- and E_+ bands (see table 3). The value of the g-factor for Γ_7, $g^*_{\Gamma 7} = -4.9 \pm 0.6$, is very close to that measured for GaAs [18].

We would like to emphasize here that the electron g-factor for the E_- band ($g^*_{E-} = -0.7 \pm 0.2$) has an opposite sign to that for the E_+ band ($g^*_{E+} = +2.8 \pm 0.8$).

Three-or five-band $k \cdot p$ models for III–V and II–V compounds indicate that the conduction band g-factor equals $g_e^* = g_0 + A_{SO} + C$, where $g_0 = 2$ is the free-electron Landé g-factor, A_{SO} is related to the spin–orbit interaction, and C represents far-band contribution. The A_{SO} term depends on the relative positions of conduction and valence bands, and in all III–V and II–V compounds is always negative [14–16]. The C constant, negligible in comparison

with A_{SO}, is equal to -0.04 [14–16]. Due to the term related to the spin–orbit interaction, the effective g-factor in almost all III–V compounds is smaller than 2 (e.g., $g_e^* = 1.26$ for InP [15]) and becomes smaller and smaller, and even negative, as the fundamental gap shrinks (e.g., $g_e^* = -51$ for InSb [15]). On this basis, a decrease of the g-factor for the E_- band for higher N content can be understood as resulting from a shrinkage of the energy gap with increase of the nitrogen content. The positive value of the g-factor for the E_+ band can result from two reasons. First, A_{SO} can be negligible (the distance between E_+ and the valence bands is large). Second, this may be an effect of the contribution of the N-related states to the E_+ band. We note here that the electron effective g^*-factor for GaN is equal to about 2 [23].

4.4. The electron effective mass at the bottom of the E_- band

In general, oscillations of the amplitude of the circular dichroism (figure 6) or the FR angle versus energy (figure 7) can originate from transitions between the valence and the conduction band Landau levels or magneto-exciton transitions. In the latter case, one deals with excitonic states split in the magnetic field and transitions that take place according to appropriate selection rules. As can be inferred from [21] and [22], magneto-exciton transitions are characterized by a nonlinear energy on the magnetic field strength dependence (including the exciton diamagnetic shift), a sharpness of lines and splitting of the order of tens of millielectronvolts (0.2–0.3 meV for 5 T). This is not the case of the structures observed in our FR experiment that show a linear dependence on the magnetic field and a characteristic energy scale of the order of a few millielectronvolts (14 meV for 5 T—see the inset to figure 6). Because of this, we analyse the oscillation of the FR angle assuming that they originate only from the quantization of the bands into the Landau levels, neglecting magneto-exciton corrections. The quantization of the conduction band density of states into the Landau levels is described by equation (1); a similar equation can be written for the valence band.

In figure 11 we plot the positions of the FR angle minima for different magnetic fields. The linear behaviour of this fan chart of lines intersecting in one point at $B = 0$ is an argument for the Landau level splitting. From this plot we can derive a reduced effective mass, μ_R, composed by the electron and the hole effective mass:

$$\frac{1}{\mu_R} = \frac{1}{m_e^*} + \frac{1}{m_h^*}. \tag{7}$$

The dashed lines in figure 11 are plotted for $\mu_R = 0.042\, m_0$. This value is slightly smaller than the one measured for GaAs ($0.048\, m_0$) [22]. Now, we can estimate the effective mass of the electrons. There are two possibilities: the initial state for the optical transition can be related either with the heavy or with the light holes. For the heavy holes ($m_{hh}^* = 0.45\, m_0$) we get $m_e^* = 0.046\, m_0$, and for the light holes we get $m_e^* = 0.086\, m_0$. In the context of the discussion about the presence of strain in the investigated layer, we can assume that the light hole valence band is above the heavy hole band. This suggests that the electron effective mass is equal to $0.086\, m_0$ for 1% N and 4% In GaInNAs. This value fits well with other experimental and theoretical findings [9, 24, 25]. However, we would like to stress here that a systematic study of the effective mass at the bottom of the E_- band in GaInNAs is still missing. The main reason is that in these new alloys the electron mobility is very low (in the range of 100–600 $cm^2\ V^{-1}\ s^{-1}$), making experiments that give the value of the effective mass directly, like cyclotron resonance or Shubnikov–de Haas effect measurements, very difficult to perform.

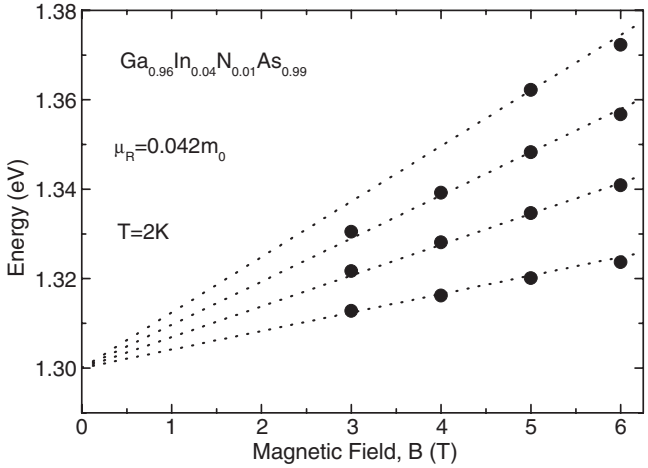

Figure 11. The minima observed in the Faraday rotation as a function of magnetic field. The dotted lines are positions of energy transitions from the valence band Landau levels to the conduction band Landau levels, calculated for a reduced effective mass $\mu_R = 0.042\ m_0$.

5. Conclusions

In this paper we report for the first time the value for the electron and hole g-factors in $Ga_{0.96}In_{0.04}N_{0.01}As_{0.99}$ for the E_- ($g^*_{E-} = -0.7 \pm 0.2$), E_+ ($g^*_{E+} = +2.8 \pm 0.8$), Γ_7 ($g^*_{\Gamma 7} = -4.9 \pm 0.6$), and Γ_8 ($g^*_{\Gamma 8} = -1.6 \pm 0.2$) bands. We study the nitrogen and indium content dependence of the electron effective g-factor for the E_- band. We provide arguments for the presence of strain in one of our layers ($Ga_{0.96}In_{0.04}N_{0.01}As_{0.99}$ mounted on sapphire) that lifts the light hole–heavy hole degeneracy at the top of the Γ_8 valence band. Oscillations of the FR angle versus energy (observed on this sample) enabled us to deduce the electron–hole reduced effective mass: $\mu_R = 0.042\ m_0$. The electron effective mass, $m^*_e = 0.086\ m_0$, at the bottom of conduction band for $Ga_{0.96}In_{0.04}N_{0.01}As_{0.99}$ is inferred when assuming the light hole contribution to the reduced mass.

Acknowledgments

We are thankful to D E Mars and J F Geisz for providing samples used in present study, to W Mac for his help in magneto-optical experiments and J Gaj for stimulating discussions.

References

[1] Uesugi K, Marooka N and Suemune I 1999 *Appl. Phys. Lett.* **74** 1254
[2] Shan W, Walukiewicz W, Ager J W III, Haller E E, Geisz J F, Friedman D J, Olson J M and Kurz S R 1999 *Phys. Rev. Lett.* **82** 1221
[3] Perlin P, Wiśniewski P, Skierbiszewski C, Suski T, Kamińska E, Subramanya S G, Weber E R, Mars D E and Walukiewicz W 2000 *Appl. Phys. Lett.* **76** 1279
[4] Skierbiszewski C, Perlin P, Wiśniewski P, Suski T, Geisz J F, Hingerl K, Jantsch W, Mars D and Walukiewicz W 2002 *Phys. Rev.* B **65** 35207
[5] Skierbiszewski C, Perlin P, Wiśniewski P, Knap W, Suski T, Walukiewicz W, Shan W, Ager J W, Haller E E, Geisz J F, Friedman D J, Olson J M and Kurtz S R 2000 *Appl. Phys. Lett.* **76** 2409
[6] Szwacki G and Bogusławski P 2001 *Phys. Rev.* B **64** 161201
[7] Kent P R C and Zunger A 2001 *Phys. Rev. Lett.* **86** 2609

[8] Bellaiche L, Modine N A and Jones E D 2000 *Phys. Rev.* B **62** 15311
[9] Gorczyca I, Skierbiszewski C, Suski T, Christensen N E and Svane A 2002 *Phys. Rev.* B **66** 81106
[10] Zunger A 1999 *Phys. Status Solidi* b **216** 117
[11] Shan W, Walukiewicz W, Yu K M, Ager J W III, Haller E E, Geisz J F, Friedman D J, Olson J M, Kurtz S R, Xin H P and Tu C W 2001 *Phys. Status Solidi* b **223** 75
[12] Oestreich M and Ruhle W 1995 *Phys. Rev. Lett.* **74** 2315
[13] Weisbuch C and Herman C 1977 *Phys. Rev.* B **15** 816
[14] Roth L M, Lax B and Zwerdling S 1959 *Phys. Rev.* **114** 90
[15] Herman C and Weisbuch C 1977 *Phys. Rev.* B **15** 823
[16] Pfeffer P and Zawadzki W 1996 *Phys. Rev.* B **53** 12813
[17] Zwara M 1969 *Phys. Status Solidi* **36** 785
[18] Reine M, Aggarwal R L, Lax B and Wolfe C M 1970 *Phys. Rev.* B **2** 458
[19] Geisz J F, Friedman D J, Olson J M, Kurtz S R and Keyes B M 1998 *J. Cryst. Growth* **195** 401
[20] Perlin P, Subramanya S G, Mars D E, Kruger J, Shapiro N A, Siegle H and Weber E R 1998 *Appl. Phys. Lett.* **73** 3703
[21] Willmann F, Suga S, Dreybrodt W and Cho K 1974 *Solid State Commun.* **14** 783
[22] Nam S B, Reynolds D C, Litton C W, Almassy R J, Collins T C and Wolfe C M 1976 *Phys. Rev.* B **13** 761
[23] Rodina A V, Dietrich M, Goldner A, Eckey L, Efros Al L, Rosen M, Hoffmann A and Meyer B K 1999 *Phys. Status Solidi* b **216** 21
[24] Hai P N, Chen W M, Buyanova I A, Xin H P and Tu C W 2000 *Appl. Phys. Lett.* **77** 1873
[25] Skierbiszewski C, Łepkowski S P, Perlin P, Suski T, Jantsch W and Geisz J 2002 *Physica* E **13** 1078